

RSC Advances



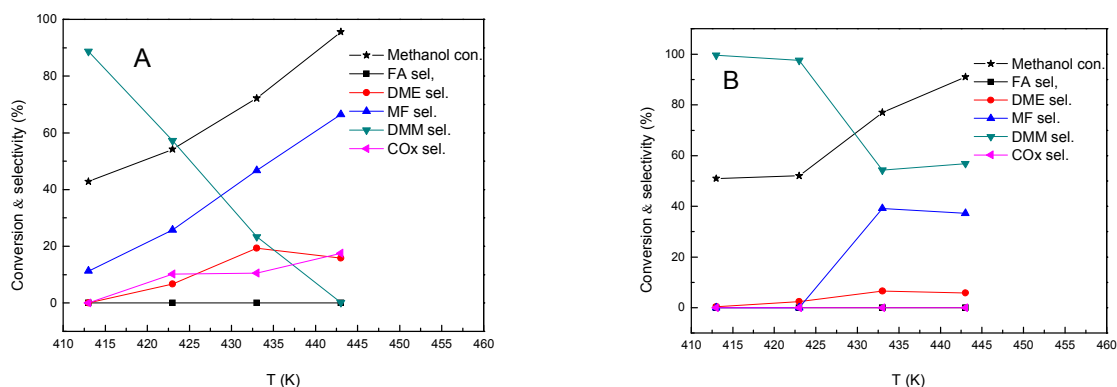
This is an *Accepted Manuscript*, which has been through the Royal Society of Chemistry peer review process and has been accepted for publication.

Accepted Manuscripts are published online shortly after acceptance, before technical editing, formatting and proof reading. Using this free service, authors can make their results available to the community, in citable form, before we publish the edited article. This *Accepted Manuscript* will be replaced by the edited, formatted and paginated article as soon as this is available.

You can find more information about *Accepted Manuscripts* in the [Information for Authors](#).

Please note that technical editing may introduce minor changes to the text and/or graphics, which may alter content. The journal's standard [Terms & Conditions](#) and the [Ethical guidelines](#) still apply. In no event shall the Royal Society of Chemistry be held responsible for any errors or omissions in this *Accepted Manuscript* or any consequences arising from the use of any information it contains.

Graphical Abstract



The figures above presented the catalytic performances of V_2O_5/TiO_2 (A) and composite supported $V_2O_5-TiO_2-SiO_2$ (B) catalysts prepared by improved sol-gel method. Sample V_2O_5/TiO_2 exhibited methanol conversion of 43% of and DMM selectivity of 89% at 413 K. Sample $V_2O_5-TiO_2-SiO_2$ showed efficient activity of 51% methanol conversion and DMM selectivity of 99% among all samples at 413 K. Results showed more weak acids and more Brønsted acids, higher active surface oxygen species on $V_2O_5-TiO_2-SiO_2$ catalyst facilitated its catalytic performance.

Efficient V_2O_5/TiO_2 composite catalysts for dimethoxymethane synthesis from methanol selective oxidation

Zhihong Fan^{a,b,c}, Heqin Guo^a, Kegong Fang^{a,*}, Yuhan Sun^{d,*}

^a State Key Laboratory of Coal Conversion, Institute of Coal Chemistry, Chinese Academy of Sciences, Shanxi, Taiyuan 030001, P. R. China

^b University of Chinese Academy of Sciences, Beijing, 100049, P. R. China

^c Shanxi Agricultural University, Shanxi, Taigu, 030801, P. R. China

^d Low Carbon Conversion Center, Shanghai Advanced Research Institute, Chinese Academy of Sciences, Shanghai, 201203, P. R. China

Abstract

A series of V_2O_5/TiO_2 composite catalysts ($V_2O_5-TiO_2-Al_2O_3$, $V_2O_5-TiO_2-SiO_2$, $V_2O_5-TiO_2-Ce_2O_3$ and $V_2O_5-TiO_2-ZrO_2$) were prepared by improved rapid sol-gel method and the catalytic behavior for dimethoxymethane (DMM) synthesized from methanol selective oxidation was investigated. The physicochemical properties of catalysts were characterized by X-ray diffraction (XRD), Brunauer-Emmett-Teller isotherms (BET), X-ray photoelectron spectroscopy (XPS), Hydrogen temperature-programmed reduction (H_2 -TPR), NH_3 temperature programmed desorption (NH_3 -TPD), Infrared spectroscopy of adsorbed pyridine (Py-IR) and transmission electron microscopy (TEM) techniques. The best catalytic performance was obtained on $V_2O_5-TiO_2-SiO_2$ catalyst with methanol conversion of 51% and DMM selectivity of 99% at 413 K. Furthermore, the $V_2O_5-TiO_2-SiO_2$ catalyst displayed an excellent catalytic stability within 240 h. Results showed that more Brønsted acidic sites were

*Corresponding author. Tel.: +86 351 4040431, E-mail: kgfang@sxicc.ac.cn (K. Fang); yhsun@sxicc.ac.cn, yhsun@sari.ac.cn (Y. Sun).

critical to increasing the DMM yield. The activity of V_2O_5/TiO_2 composite catalysts decreased with increasing of Brønsted acidity, but the yield of DMM increased with rising of amount of Brønsted acidic sites. The excellent performance of $V_2O_5-TiO_2-SiO_2$ catalyst might come from its optimal acidity and redox property, higher active surface oxygen species, together with more Brønsted acids.

Keywords: V_2O_5/TiO_2 composite catalysts; Methanol selective oxidation; Dimethoxymethane

1. Introduction

Dimethoxymethane (DMM), a low toxicity chemical reagent and a valuable methanol downstream product, is widely used as efficient diesel fuel additive as well as an excellent solvent in pharmaceutical and perfume industries [1-4]. DMM can be synthesized from the selective oxidation of methanol ($3\text{CH}_3\text{OH} + 1/2\text{O}_2 \rightarrow \text{CH}_3\text{OCH}_2\text{OCH}_3 + 2\text{H}_2\text{O}$), which may relieve the problem of methanol surplus from coal-derived syngas [5-7].

In recent years numerous efforts have been devoted to the selective oxidation of methanol to obtain DMM [8-10]. In these reports, two types of active sites in catalysts, including both redox sites and acidic sites, were required for DMM synthesis [11]. The redox sites were considered to be involved in the initial formation of formaldehyde (FA) from CH_3OH with active lattice oxygen atoms, while acidic sites can catalyze acetalization reactions of FA and CH_3OH to DMM. However, methyl formate (MF) could also be produced on redox sites and acidic sites favored another side product of dimethyl ether (DME). Therefore, both the redox property and acidity of catalyst are needed and should match each other in order to obtain DMM with high selectivity.

It was reported that $\text{V}_2\text{O}_5/\text{TiO}_2$ -based (VT-based) catalysts exhibited excellent activity for the selective oxidation of methanol to DMM in mild reaction conditions [12]. However, the physiochemical properties and catalytic performance of VT-based catalysts were influenced greatly by several factors, especially the preparation method and support additives [13-16]. Traditionally, the VT-based catalysts can be prepared by incipient wetness impregnation [17-20], co-precipitation [21] and rapid combustion method [22]. In these methods, an additional heat treatment was typically required to obtain the desired phase composition,

which usually led to a significant aggregation of catalyst particles. The aggregated catalyst particles might weaken the interaction between vanadium and supports, leading to low reducibility [23, 24], which was unfavorable for the first step of DMM synthesis [25, 26]. Moreover, this aggregation might also decrease the number of acidic sites [25], harmful for the second step for DMM synthesis [27]. Generally, the addition of some elements to the support may decrease the aggregation of catalyst particles in some extent. For example, the addition of Al, Si, Ce and Zr to V_2O_5/TiO_2 catalyst may affect both redox and acidic properties and dispersion of the active phase [21, 28 and 29]. However, these catalysts were prepared mainly by co-precipitation or incipient wetness impregnation, which may cause the particles aggregation or the metal nonuniform distribution. These may cause the selectivity to DMM usually decreased sharply with the increase of methanol conversion over traditional V_2O_5/TiO_2 catalysts, leading to a low DMM yield [30]. Thus, it is necessary to develop new catalyst with improved preparing method for the selective oxidation of methanol to obtain DMM efficiently from the point of scientific significance and economic view.

In this article, we designed an improved rapid sol-gel method, which overcame the demanding and not easy to control of traditional sol-gel method, avoided the deficiency of the above methods and evenly combined the metals on molecular level, to prepare the composite supported V_2O_5/TiO_2 catalysts ($V_2O_5-TiO_2-Al_2O_3$, $V_2O_5-TiO_2-SiO_2$, $V_2O_5-TiO_2-Ce_2O_3$ and $V_2O_5-TiO_2-ZrO_2$) and get bifunctional catalysts with high DMM selectivity and high methanol conversion simultaneously and excellent life span in methanol selective oxidation. The changed dispersity of vanadium, redox and acid properties of the catalysts prepared by improved sol-gel method with stable three dimensional structures would affect the catalytic

property apparently. The physiochemical properties of the catalysts were characterized exhaustively together with the catalytic performance investigation.

2. Experimental section

2.1. Catalyst preparation

The composite supported V_2O_5/TiO_2 catalysts were prepared by improved rapid sol-gel method, including the following steps. 2 g NH_4VO_3 and the calculated amount of citric acid were dissolved in 100 mL deionized water under vigorous stirring to form vanadium-containing solution (S1). 4 mL $TiCl_4$ was rapidly transferred to 100 mL of 6 mol/L HCl using pipet under stirring and then the calculated amount of citric acid was added to the solution to form titanium-containing solution (S2). The oxide-support precursor ($Al(NO_3)_3$, or TEOS, or $Ce(NO_3)_3$, or $ZrOCl_2$), and the corresponding amount of citric acid were dissolved into a limited deionized water under constantly stirring to form the metal ion containing solution (S3). The S2 and S3 were slowly dropped into S1 in turn under continuous stirring to form a precipitation. The precipitate was aged for 1 h at 373 K under stirring in air to form a transparent sol. Then, the sample was dried for 5 h at 393 K, followed by calcination at 673 K for 6 h to remove the organic materials. The obtained catalysts were denoted as $V_2O_5-TiO_2-Al_2O_3$ (VTiAl), $V_2O_5-TiO_2-SiO_2$ (VTiSi), $V_2O_5-TiO_2-Ce_2O_3$ (VTiCe) and $V_2O_5-TiO_2-ZrO_2$ (VTiZr). The theoretical amount of vanadium pentoxide of all samples was fixed at 15 wt% whatever the other metal oxide used. The weight ratio between the TiO_2 and metal oxide (Al_2O_3 , SiO_2 , Ce_2O_3 or ZrO_2) supports was 1:1. The molar ratio between the total amount of metals (V, Ti, Al, Si, Ce or Zr) and citric acid was 1:0.6.

For comparison, the V_2O_5/TiO_2 (VTi) catalyst, containing the same vanadium content denoted as VTi, was prepared by the same method.

2.2 Catalyst characterization

X-ray diffraction (XRD) patterns were measured on a Bruker Advanced X-ray Solutions/D8-Advance scanning from 3° to 85° (2θ) at a rate of $0.02^\circ/s$ using a $Cu\ K\alpha_1$ radiation ($\lambda=0.15418\text{ nm}$) source. The applied voltage and current were 50 kV and 35 mA, respectively.

Measurements of the BET surface area and pore volume of catalysts were performed in a Micromeritics ASAP-2000 instrument by N_2 adsorption-desorption. Before analysis, the samples were degassed at 473 K overnight.

The elemental analysis was carried out using ICP optical emission spectroscopy (ICP-OES) with an ACTIVA spectrometer from Horiba JOBIN YVON.

X-ray photoelectron spectroscopy spectra (XPS) were recorded on a XSAM-800 spectrometer using an $Al\ K\alpha$ (1486.7 eV) X-ray source.

Infrared spectroscopy of adsorbed pyridine (Py-IR) was applied to determine the kinds of surface acid and the measurements were performed in a Nicolet Magna 550 spectrophotometer. Wafers of $15\text{ mg}\cdot\text{cm}^{-2}$ were degassed overnight under vacuum (10^{-3} Pa) at 673 K for 1 h and then saturated by pyridine. Samples were evacuated to eliminate the physically adsorbed pyridine for 30 min. The amount of Brønsted and Lewis acid sites was calculated from the intensities of the IR bands at ca. 1540 cm^{-1} and 1450 cm^{-1} , respectively.

Transmission electron microscopy (TEM) images were recorded using a JEOL-2011 microscope operated at 200 kV.

NH₃ temperature programmed desorption (NH₃-TPD) was performed in a quartz micro-reactor. 200 mg of each sample was heated in Ar at 773 K for 2 h, then NH₃ was introduced to the sample after the sample was cooled down to 353 K under Ar flow. After the sample was swept using Ar at 353 K for 1 h to remove the weakly adsorbed NH₃, the TPD experiments were carried out with a carrier gas at a flow of 40 mL·min⁻¹ Ar and the TPD spectra were recorded using a linear heating rate of 10 K·min⁻¹ from 353 K to 900 K by a Shanghai GC-920 equipped with a thermal conductivity detector (TCD). The desorbed NH₃ was titrated by 0.01 mol/L HCl. The amount of desorbed NH₃ was corresponding to the total number of acidic sites. The acidity intensity could be determined according to the desorption temperature of NH₃, and the number of acidic sites can be calculated based on the areas of desorption peaks.

Hydrogen temperature-programmed reduction (H₂-TPR) was carried out with a mixture of 5% H₂/N₂ as the reductive gas. A sample of about 200 mg was reduced in a flow of H₂/N₂ at a heating rate of 10 K·min⁻¹ from room temperature to 1000 K. The effluent gas was detected by TCD after the removal of produced water using 5Å molecular sieves.

2.3 Catalytic test and analytic procedure

The selective oxidation of methanol was carried out in a fixed bed micro reactor at atmospheric pressure. About 0.8 g of catalyst sample (40-60 mesh) diluted with quartz sand with the same size and volume. After the sample was activated at 673 K for 1 h in a flow of 10% O₂/Ar (70 mL·min⁻¹) and cooled down to the reaction temperature, the gasified methanol (99.9%) was introduced into the reaction zone. The gas hourly space velocity (GHSV) was 12,000 mL·g_{cat}⁻¹·h⁻¹. The feed composition was maintained at Ar: O₂: methanol = 84.15: 9.35:

6.50 (v/v). The reaction products were analyzed by an on-line gas chromatography (GC-950) using a Propack T column and a TDX-01 column connected to TCD detector and FID detector, respectively. The gas lines were kept at 393 K to prevent condensation of the reactant and products.

The product selectivity was calculated on carbon molar base:

$$S_i = Y_i n_i / \sum Y_i n_i \times 100\%$$

Wherein, i is DMM, FA, DME, MF and CO_x , S_i is the selectivity of product i , Y_i is the number of carbon atom of product i , and n_i is the molar of product i .

3. Results

3.1 Physico-chemical characterization

Fig.1 shows the XRD patterns of VTi, VTiAl, VTiSi, VTiCe and VTiZr catalysts. As can be seen, the typical diffraction peaks characteristic of anatase TiO_2 appeared for VTi, VTiAl, VTiSi, and VTiCe samples [31]. Whereas, sample VTiZr exhibited much broader diffraction peaks indicating more amorphous nature. This was relevant with the catalyst calcination temperature [32]. Most importantly, no lines due to crystalline V_2O_5 were seen in the spectra. This observation clearly indicated that vanadium oxide was present in a highly dispersed [32]. The crystalline V_2O_5 was detected on VTiCe and VTiAl catalyst. For the other catalysts, no crystalline V_2O_5 was observed, implying that the vanadium was highly dispersed on TiO_2 or the V_2O_5 crystalline was less than 4 nm (beyond the detection capacity of the power XRD technique) [33].

In order to confirm the dispersion of vanadium, the surface and bulk composition of the prepared samples were studied by XPS and ICP techniques (see Table 1). The bulk vanadium contents were similar for all the catalysts. The surface vanadium on VTiSi, VTiZr and VTi catalysts was higher than that of bulk, suggesting the vanadium oxide was mainly dispersed on the surface of the catalysts. However, the surface vanadium on VTiCe and VTiAl catalysts was lower than those in the bulk, indicating that the vanadium mainly existed on the bulk of the catalysts. Calculation shows that V atom numbers per nm^2 on VTi catalyst was 5.6, which agrees well with the report that 7-8 V atoms per nm^2 was required to form the monolayer-dispersion [34]. The values were only 3.6 and 6.4 on VTiSi and VTiZr catalysts, respectively, inferring the high dispersed V species which were half less than the theoretical value. However, the values were 16.5 for VTiCe catalyst, which was almost two times larger than the theoretical value, because of its low surface area. And the values were 11.5 for VTiAl catalyst, which was larger than the theoretical value too. Thus the crystalline V_2O_5 appeared as confirmed by XRD measurement.

The isotherms of all samples in Fig. S1 showed the type of IV with the hysteresis loops at relative pressures of 0.4-1.0, which was characteristic for mesoporous materials [35]. The pore size distribution for VTi, VTiCe and VTiZr catalysts, centered at about 3.5 nm, while the peak centered at 5.3 and 9.0 nm appeared for VTiSi and VTiAl catalyst respectively (Table 1). The pore volume of VTiAl increased slightly to $0.25 \text{ cm}^3/\text{g}$ compared with that of VTi sample ($0.15 \text{ cm}^3/\text{g}$) while the number increased sharply to $0.55 \text{ cm}^3/\text{g}$ for VTiSi sample, which may favor the subsequent reaction. The pore volume of VTiCe, however, decreased to $0.08 \text{ cm}^3/\text{g}$ while that of VTiZr kept almost unchanged.

Table 2 showed the results of binding energies and peak fitting results. The $Ti2p_{3/2}$ binding energy for all the samples were around 458 eV, which was in reasonable agreement with those for Ti^{4+} in literature [36]. The O_{1s} peak showed two types of oxygen species. The binding energy around 530.8 eV was the characteristic of lattice oxygen species of TiO_2 and V_2O_5 , and the binding energy at 532.3 eV could be attributed to active surface oxygen species, including surface oxygen of adsorbed oxygen species, weakly bonded oxygen and hydroxyl-like groups [37-40]. Sample VTiSi had much more active oxygen than others. The reference $V2p_{3/2}$ peak positions for V_2O_5 and V_2O_4 were around 517.4 and 516.3 eV, respectively [41, 42]. The full oxidation state of V^{5+} was predominant at catalyst surface. It was clearly seen that a greater amount of V^{4+} species was presented on the VTiSi surface than that of others, indicating that the degree of reduction of V_2O_5 was enhanced with the Si addition.

The morphology was characterized by the TEM techniques (Fig. 2). It was found that the particles size of VTi was only 5-6 nm. The particle size increased apparently with the addition of Al, Si, Ce and Zr. Such as the particle size of sample VTiAl, VTiSi, VTiCe and VTiZr were about 190, 390, 260 and 200 nm, respectively. Metal additives affected the combination of vanadium and titanium.

3.2 Acid properties

Acidity was one of the most significant surface properties for the selective oxidation of vanadium-based catalysts [43]. The acidity of the samples was measured by NH_3 adsorption experiments (see Fig. 3 and Table 3). As it could be seen, two peaks of NH_3 absorption could be identified in the temperature range of 380-530 K, which could be attributed to weak acidic

site and middle strong acidic sites, respectively. The desorption peak at low temperature of 380-450 K might be related to the physisorbed NH_3 or weak acidic sites, while desorption peak at high temperature of 450-530 K might be attributed to the strong acidic sites [20] [44]. Table 3 showed that the calculated acid sites with weak and middle strength were 462 and 162 $\mu\text{mol g}^{-1}$ on VTi catalyst, respectively. The addition of Si to VTi catalyst increased the number of both weak acid sites and middle strong acid sites. However, with the addition of Al, Ce and Zr, the acid sites decreased. The increased acid sites for VTiSi might improve its oxidation activity for methanol to DMM.

Chemisorption of pyridine followed by FTIR spectroscopy was useful to probe the presence and nature of surface acid sites on catalysts [45, 46]. Table 3 showed that VTiSi catalyst exhibited larger amount of Brønsted acidic sites and less Lewis acidic sites compared with those of VTiAl, VTiCe and VTiZr catalysts. Combined to the NH_3 -TPD results, adding Si element to VTi catalyst brought more acid sites which mainly were Brønsted acidity. However, the addition of Al, Zr and Ce element to VTi catalyst resulted in smaller amount of acid sites since the weak interaction between V and supports.

3.3 Redox properties

The redox properties of the prepared samples were measured by the H_2 -TPR techniques (Fig. 4). It was usually reported that the reducibility of vanadium-based catalysts could be greatly influenced by the existing state of vanadium [47]. As shown in Fig. 4, two H_2 consumption peaks at about 705 K and 793 K were observed on VTi catalyst, which were attributed to the reduction of the highly dispersed surface vanadium species [48]. The H_2 consumption peaks around 863 K and 977 K were attributed to the reduction of bulk V_2O_5 [49,

50]. This was attributed to the following reduction sequence: $V_2O_5 \rightarrow V_6O_{13}$ (863 K) and $V_6O_{13} \rightarrow V_2O_4 \rightarrow V_2O_3$ (977 K). VTiSi catalyst had a similar but enhanced H_2 consumption peak around 703 K which indicated the increasing reducibility of the catalyst. The fact that VTiSi can be reduced in lower temperature but with larger amount shows that this catalyst could give out crystal O_2 easier, as a result, methanol could be oxidized easier. Compared to VTi catalyst, the low reduction peak at about 776 K and high reduction peak at about 977 K shifted to higher temperature on VTiAl, VTiCe and VTiZr catalysts, shown the weak reducibility.

3.4 Catalytic activities

It was reported that the selective oxidation of methanol to DMM involves two steps: (1) Oxidation of methanol to FA on redox sites, and (2) Condensation of the produced FA with additional methanol to form DMM on acidic sites [15]. So the selective oxidation of methanol was very sensitive to the catalysts of the surface acidity and redox properties [4]. The catalytic test showed that the reducibility and oxidizability of catalyst determines its catalytic activity [51].

Table 4 presented the catalytic performances of composite supported V_2O_5/TiO_2 catalysts. The sample VTi exhibited a highest methanol conversion of 43% of and a DMM selectivity of 89% at 413 K. The selectivity for MF was 10% and 1% for DME. The distribution of products on VTi catalyst indicated the surface acidity was not strong enough to effectively catalyze the reaction of FA condensation with methanol to produce DMM, leading to the production of MF and a small amount of DME. The methanol conversion increased sharply with increasing reaction temperature, meanwhile, the selectivity to DMM decreased while the selectivity to

MF and DME increased. The sudden drop in DMM selectivity possibly came from the thermodynamic constrains for DMM synthesis [52].

Compared to VTi catalyst, sample VTiSi showed the highest activity of 51% methanol conversion and DMM selectivity of 99% among all samples at 413 K. Moreover, when the temperature increased to 423 K, the DMM selectivity was still kept at 98% with the methanol conversion of 52%. In addition, the stability was carried for VTiSi catalyst at 413 K (Fig. 5). The result showed that DMM selectivity (99%) and methanol conversion (51%) did not change obviously within 240 h, indicating that the VTiSi catalyst exhibited an excellent stability, which probably related to its bigger particle size. All the catalytic data were better than those data shown in literature [10, 11, 23, 30 and 53].

However, sample VTiAl showed low activity for DMM synthesis from methanol selective oxidation, 23% of methanol conversion and 56% of DMM selectivity at 413 K. After the ZrO₂ doping, the VTiZr sample showed increased DMM selectivity but much lower methanol conversion compared with those of VTiSi sample. In fact, the methanol conversion kept about 28% on VTiZr catalyst when reaction temperature increased from 413 K to 423 K, the DMM selectivity exceeded 99% at 413-423 K and 92% at 433-443 K. The catalytic performance of VTiCe showed a high DMM selectivity (98%) but lowest methanol conversion (15%) was obtained.

4. Discussion

4.1 Effect of weak Brønsted acidic sites

From the NH_3 -TPD results shown in Fig. 3 and Table 3, the composite TiO_2 - SiO_2 influenced the catalytic performances by providing the necessary acidic sites and promoting create a balance for the appreciate acidic and redox sites. It could be seen that the addition of Si species to VTi catalyst could produce more weak acidic sites. Moreover, the partial reduced V-Ti mixed oxides resulted in an increased number of Brønsted acidic sites on VTiSi catalyst as shown in the FTIR spectra of pyridine absorption analysis (Table 3). The reactivity and distribution of acidic sites revealed that the DMM yield was directly proportional to the surface density of the Brønsted acidic sites on VTiSi catalyst, which accounted for its highest DMM yield among these samples. It was further confirmed by the consumption of methanol data in Table 4, the activity of V-Ti-M samples decreased with increasing of Brønsted acidity, but the yield of DMM increased with rising of amount of Brønsted acidic sites and, agreement with earlier report [8, 18 and 30].

4.2 The interact effect of vanadium and composite supports on the methanol oxidation to DMM

The VTiSi catalyst exhibited better methanol conversion and DMM selectivity than VTi catalyst and other composite VTi catalysts, implying the existence of a interact effect of V and composite supports. Moreover, VTiSi catalyst behaved excellent stable catalytic performance. We proposed that the optimized redox and acidic properties of V-Ti catalyst were critical to the effectiveness of interact effect, which might due to the three dimensional structure by the improved sol-gel catalyst preparation method. With the addition of Si, the partially reduced V-Ti species introduced an increase amount of oxygen vacancies, which improved the

adsorption capability of gaseous oxygen and then the refreshment of lattice oxygen, leading to an enhanced methanol conversion [54].

The coexistence of different valence states of V on composite VTi catalysts was verified by XPS (Table 2). A greater amount of V^{4+} species was presented on the VTiSi catalyst surface. Thus, the electron transfer between lattice oxygen and metal cations played a critical role in regenerating the catalyst to the original state by restoring the active lattice oxygen, in accordance with the above discussion.

5. Conclusions

In the present study, we have developed new preparation method and bifunctional V_2O_5/TiO_2 composite catalysts in methanol selective oxidation to DMM. Experimental results showed that sample VTiSi possessed most weak acidity and Brønsted acidity, yet sample VTiAl, VTiCe and VTiZr possessed few acids. The weak acidity and Brønsted acidity were identified as the reason for high DMM yield. The best catalytic performance was obtained for sample VTiSi catalyst with high activity for synthesizing of DMM from methanol selective oxidation. Particularly, the VTiSi catalyst exhibited an optimal 51% methanol conversion with a DMM selectivity of 99% at 413 K. Furthermore, the VTiSi catalyst displayed excellent catalytic stability. The effect of acidity on activity and selectivity reaction explained the high catalytic performance for methanol oxidation to DMM. The activity of V-Ti-M samples decreased with increasing of Brønsted acidity, but the yield of DMM increased with rising of amount of Brønsted acidic sites. More active surface oxygen species and greater amount of

V^{4+} species on catalyst facilitated the catalytic performance. The efficient and stable V_2O_5/TiO_2 composite catalyst was obtained through the improved sol-gel method.

Acknowledgments

The authors gratefully acknowledge the financial supports from the International Science & Technology Cooperation Project of Ministry of Science and Technology of China (No. 2012AA051002), Key Project of Natural Science Foundation of China (No. 21303241) and Key Project of Natural Science Foundation of Shanxi Province (No. 2012021005-6).

References

- [1] K. Fuji, S. Nakano, E. Fujita, *Synthesis* 1975, 4, 276.
- [2] A. Baiker, D. Monti, *J. Catal.* 1985, 91, 361.
- [3] J. Masamoto, T. Iwaisako, M. Chohno, M. Kawamura, J. Ohtake, K. Matsuzaki, *J. Appl. Polym. Sci.* 1993, 50, 1299.
- [4] J.M. Tatibouët, *Appl. Catal. A* 1997, 148, 213.
- [5] C.R. Anthony, L. Mcelwee-White, *J. Mol. Catal. A: Chem.* 2005, 227, 113.
- [6] F. Roozeboom, P.D. Cordingley, P.J. Gellings, *J. Catal.* 1981, 68, 464.
- [7] S. Damyanova, M.L. Cubeiro, J.L.G. Fierro, *J. Mol. Catal. A: Chem.* 1999, 142, 85.
- [8] S. Chen, S. Wang, X. Ma, J. Gong, *Chem. Commun.* 2011, 47, 9345.
- [9] H. Guo, D. Li, D. Jiang, H. Xiao, W. Li, Y. Sun, *Catal. Today* 2010, 158, 439.
- [10] H. Zhao, S. Bennici, J. Cai, J. Shen, A. Auroux, *J. Catal.* 2010, 272, 176.
- [11] Y. Fu, J. Shen, *Chem. Commun.* 2007, 21, 2172.
- [12] G.C. Bond, S.F. Tahir, *Appl. Catal. A* 1991, 71, 1.
- [13] L.E. Briand, R.D. Bonetto, M.A. Sanchez, H. J. Thomas, *Catal. Today* 1996, 32, 205.
- [14] M.P. Casaletto, L. Lisi, G. Mattogno, P. Patrono, F. Pinzari, G. Ruoppolo, *Catal. Today* 2004, 91/92, 271.
- [15] F. Roozeboom, T. Fransen, P. Mars, P.J. Gellings, *Z. Anorg. Allg. Chem.* 1979, 449, 25.
- [16] G.Hausinger, H.Schmelz, H.Knijzinger, *Appl. Catal.* 1988, 39, 267.
- [17] V.V. Kaichev, G.Ya. Popova, Yu.A. Chesalov, A.A. Saraev, *J. Catal.* 2014, 311, 59.
- [18] Y. Meng, T Wang, S. Chen, Y. Zhao, X. Ma, J. Gong, *Appl. Catal. B* 2014, 160, 161.
- [19] J. Cai, Y. Fu, Q Sun, M. Jia, J. Shen, *Chinese Journal of Catalysis* 2013, 34, 2110.

- [20] X. Lu, Z. Qin, M Dong, H. Zhu, J. Wang, *Fuel* 2011, 90, 1335.
- [21] H. Zhao, S. Bennici, J. Cai, J. Shen, A. Auroux, *J. Catal.* 2010, 274, 259.
- [22] H. Guo, D. Li, D Jiang, W. Li, Y. Sun, *Catal. Commun.* 2010, 1, 396.
- [23] J. Liu, Y. Fu, Q. Sun, J. Shen, *Micropor. Mesopor. Mater.* 2008, 116, 614.
- [24] Bera P, Patil KC, Jayaram V, Subbanna G. N, Hegde M. S., *J. Catal.* 2000, 196, 293.
- [25] Y. Yuan, Shido T, Iwasawa Y, *J. Phys. Chem. B* 2002, 106, 4441.
- [26] K Nishiwaki, N Kakuta, A Ueno, H Nakabayashi, *J. Catal.* 1989, 118, 498.
- [27] H. Liu, E. Iglesia, *J. Phys. Chem. B* 2005, 109, 2155.
- [28] F. Arena, F. Frusteri, A. Parmaliana, *Appl. Catal. A* 1999, 176, 189.
- [29] L. Owens, H.H. Kung, *J. Catal.* 1993, 144, 202.
- [30] G. Busca, A. S. Elmi, P. Forzatti, *J. Phys. Chem.* 1987, 91, 5263.
- [31] M.A. Bañares, L.J. Alemany, M.C. Jimen'ez, M.A. Larrubia, F. Delgado, M.L. Granados, A.M. Arias, J.M. Blasco, J.G. Fierro, *J. Solid State Chem.* 1996, 124, 69.
- [32] Benjaram M. Reddy, Biswajit Chowdhury, Ibram Ganesh, *J. Phys. Chem. B* 1998, 102, 10176.
- [33] Q. Sun, Y. Fu, J. Liu, A. Auroux, J. Shen, *Appl. Catal. A* 2008, 334, 26.
- [34] I.E. Wachs, B.M. Weckhuysen, *Appl. Catal. A* 1997, 157, 67.
- [35] M. Kruk, M. Jaroniec, C.H. Ko, R. Ryoo, *Chem. Mater.* 2000, 12, 1961.
- [36] J. Keränen, C. Guimon, E.I. Iiskola, A. Auroux, L. Niinistö, *Catal. Today* 2003, 78, 149.
- [37] S. Chenakin, R. Prada Silvy, N. Kruse, *J. Phys. Chem. B* 2005, 109, 14611.
- [38] X. Huang, J. Liu, J. Chen, Y. Xu, W. Shen, *Catal. Lett.* 2006, 108, 79.
- [39] W. Xingyi, K. Qian, L. Dao, *Appl. Catal. B: Environ.* 2009, 86, 166.

- [40] K. Routray, W. Zhou, C.J. Kiely, W. Grünert, I.E. Wachs, *J. Catal.* 2010, 275, 84.
- [41] S.L.T. Andersson, *J. Chem. Soc., Faraday Trans. I* 1979, 75, 1356.
- [42] J.A. Odriozola, J.Soria, G.A. Somorjai, H.Heinemann, J.F. Garcia de la Banda, M.Lopez Granados, J.C. Conesa, *J. Phys. Chem.* 1991, 95, 240.
- [43] A.Auroux, *Top. Catal.* 1997, 4, 71-89.
- [44] L. K. Boudali, A. Ghorbel, P. Grange, F. Figueras, *Appl. Catal. B* 2005, 59, 105.
- [45] H. Miyata, Y. Nakagawa, S. Miyagawa, Y. Kubokawa, *J. Chem. Soc., Faraday Trans. I* 1988, 84, 2129.
- [46] J. Datka, A.M. Turek, J.M. Jehng, I.E. Wachs, *J. Catal.* 1992, 135, 186.
- [47] L.Briand, L.Gambaro, H. Thomas, *J. Catal.* 1996, 161, 839.
- [48] S.Besselmann, C.Freitag, O.Hinrichsen and M.Muhler, *Phys Chem Chem Phys.* 2001, 3, 4633.
- [49] M.M. Koranne, J.G. Goodwin Jr., G. Marcelin, *J. Catal.* 1994, 148, 369.
- [50] H. Bosch, B.J. Kip, J.G. Van Ommen, P.J. Gellings, *J. Chem. Soc. Faraday Trans.* 1984, 80, 2479.
- [51] M. Badlani, I.E. Wachs, *Catal. Lett.* 2001, 75, 137.
- [52] H C Liu, E. Iglesia, *J. Catal.* 2004, 223, 161.
- [53] Keyan Li, Dongfeng Xue, *J. Phys. Chem. A* 2006, 110, 11332.
- [54] O. Ovsitser, Y. Uchida, G. Mestl, G. Weinberg, A. Blume, J. Jäger, M. Dieterle, H. Hübster, R. Schlögl, *J. Mol. Catal. A: Chem.* 2002, 185, 291.

Table 1 Textural properties and chemical analysis of the catalysts.

Table 2 Peak-fitting results of O1s, V2p_{3/2} and Ti1p_{3/2} XPS spectra.

Table 3 Acid distribution of V₂O₅/TiO₂ composite catalysts.

Table 4 Catalytic activities of V₂O₅/TiO₂ composite catalysts in the methanol selective oxidation.

Fig. 1. X-ray diffraction patterns of VTi, VTiAl, VTiSi, VTiCe and VTiZr catalysts.

Fig. 2. TEM images of catalysts: (a) VTi; (b) VTiAl; (c) VTiSi; (d) VTiCe; (e) VTiZr.

Fig. 3. NH₃-TPD profiles of VTi, VTiAl, VTiSi, VTiCe and VTiZr catalysts.

Fig. 4. H₂-TPR profiles of VTi, VTiAl, VTiSi, VTiCe and VTiZr catalysts.

Fig. 5. Changes of DMM selectivity and methanol conversion with time on stream on VTiSi catalyst at 413 K.

Table 1

Sample	Texture data				Chemical composition					
	S_{BET}	Pore Volume	Pore diameter	V density	C.A. (wt %)			XPS (wt %)		
	($\text{m}^2 \cdot \text{g}^{-1}$)	($\text{cm}^3 \cdot \text{g}^{-1}$)	(nm)	calculated ^a	V	Ti	M	V	Ti	M
VTi	177	0.15	3.5	5.6	7.0	50.5	--	7.4	50.4	--
VTiAl	87	0.25	9.0	11.5	7.2	25.5	21.3	6.7	26.3	23.8
VTiSi	277	0.55	5.3	3.6	7.4	25.5	20.7	9.0	25.1	22.1
VTiCe	60	0.08	3.3	16.5	7.1	24.8	35.8	6.2	20.4	28.0
VTiZr	154	0.14	3.5	6.4	7.4	25.6	31.0	7.9	26.0	25.3

^a Supposing that all the vanadium atoms locate on the surface.

M= Al, Si, Ce, Zr.

Table 2

Sample	V2p _{3/2} (ev)		O1s (ev)		Ti2p _{3/2} (ev)	V ⁴⁺ /(V ⁴⁺ +V ⁵⁺) (Area %)	O _{sur} / (O _{sur} +O _{lat}) (Area %)
	V ⁴⁺	V ⁵⁺	O _{sur} ^a	O _{lat} ^b			
VTi	516.3	517.2	532.1	529.9	458.3	34.4	33.6
VTiAl	516.2	517.3	532.5	529.6	458.0	29.6	22.2
VTiSi	516.5	517.4	532.3	529.8	458.4	56.0	65.8
VTiCe	516.3	517.3	532.7	529.5	458.2	30.4	5.6
VTiZr	516.4	517.3	532.4	529.4	458.2	32.8	23.2

^a O_{sur} = surface active oxygen

^b O_{lat} = lattice oxygen

Table 3

Sample	Weak acidity		Middle stronger acidity		Brønsted sites/Lewis sites
	Temp.(K)	Number($\mu\text{mol g}^{-1}$)	Temp.(K)	Number($\mu\text{mol g}^{-1}$)	
VTi	414	462	503	162	0.56
VTiAl	403	323	499	198	0.37
VTiSi	387	689	477	256	0.74
VTiCe	412	147	504	96	0.38
VTiZr	384	198	480	116	0.45

Table 4

Sample	Temp.(K)	Con. of Methanol (%)	Selectivity (%)					DMM Yield	Consumption of Methanol/S _{BET}
			FA	DME	MF	DMM	CO _x		
VTi	413	43	0	1	10	89	0	38	24
	423	50	0	7	26	57	10	29	28
	433	72	0	19	47	23	11	17	41
	443	95	0	16	66	1	17	1	54
VTiAl	413	23	42	1	0	56	1	13	26
	423	24	37	3	0	58	2	14	39
	433	45	34	2	0	62	1	28	52
	443	48	31	5	0	63	1	30	55
VTiSi	413	51	0	1	0	99	0	50	18
	423	52	0	2	0	98	0	51	19
	433	77	0	7	37	56	0	43	28
	444	91	0	6	39	55	0	50	33
VTiCe	413	15	0	2	0	98	0	15	25
	423	20	0	3	0	97	0	19	33
	433	25	0	7	0	93	0	23	42
	443	30	0	7	0	93	0	28	50
VTiZr	413	28	0	1	0	99	0	28	18
	423	29	0	1	0	99	0	29	20
	433	37	2	5	0	93	0	34	24
	443	40	2	6	0	92	0	37	26

Fig. 1.

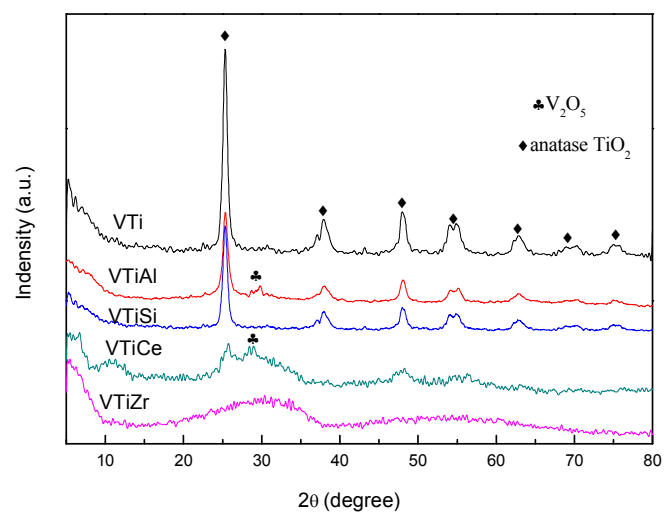


Fig. 2.

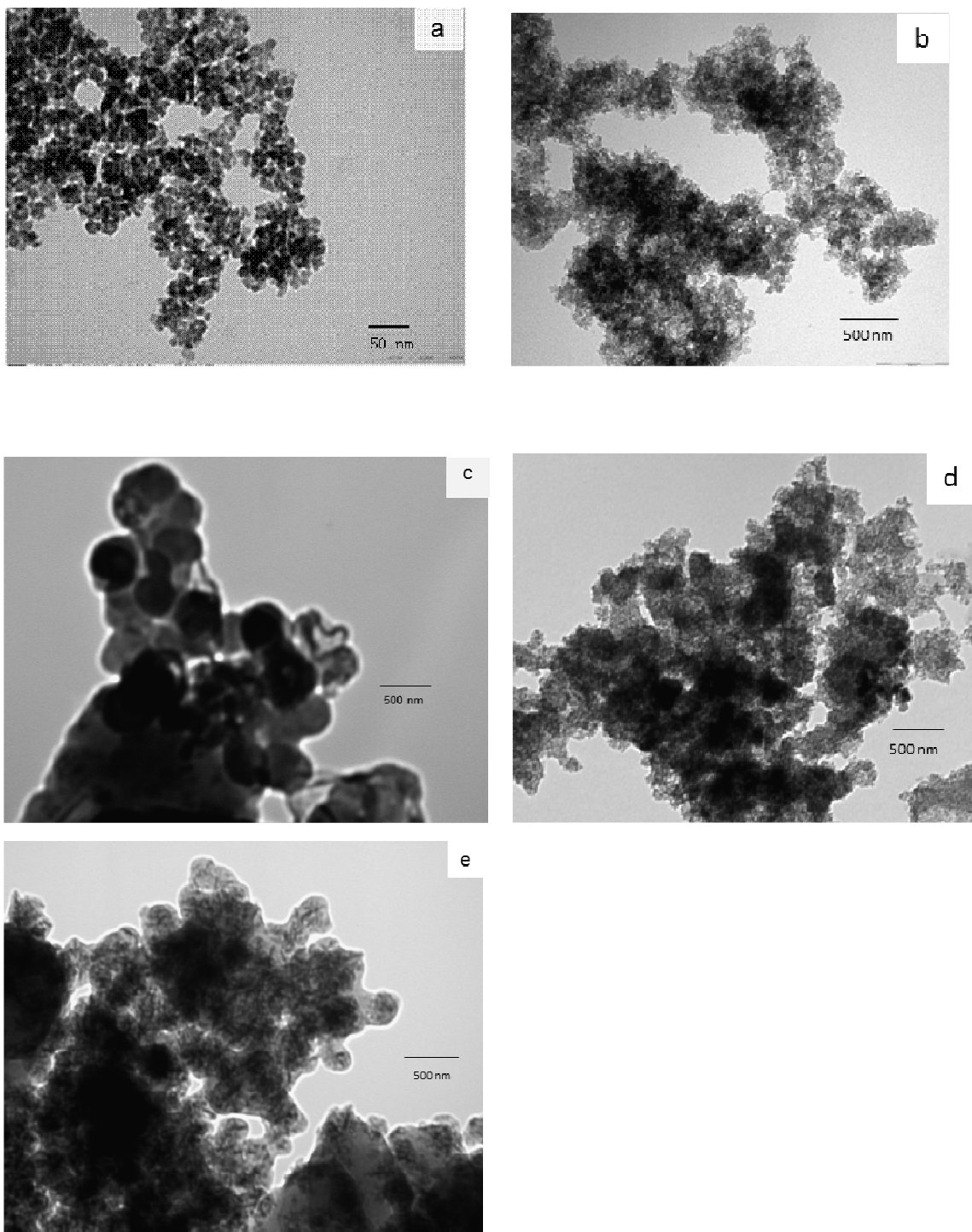


Fig. 3.

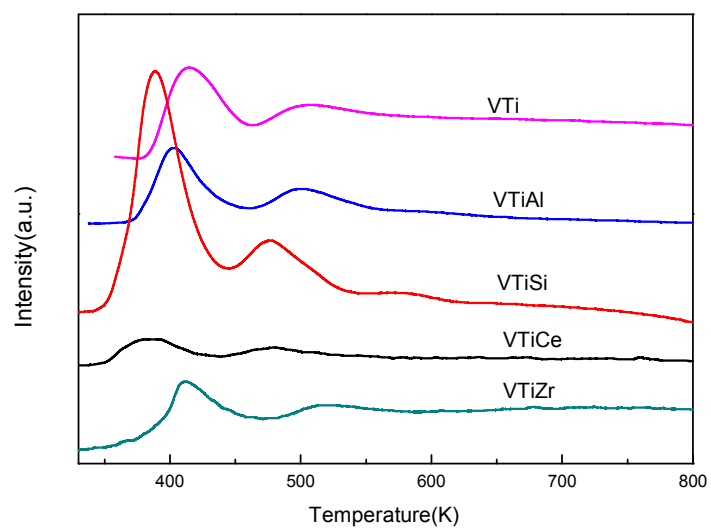


Fig. 4.

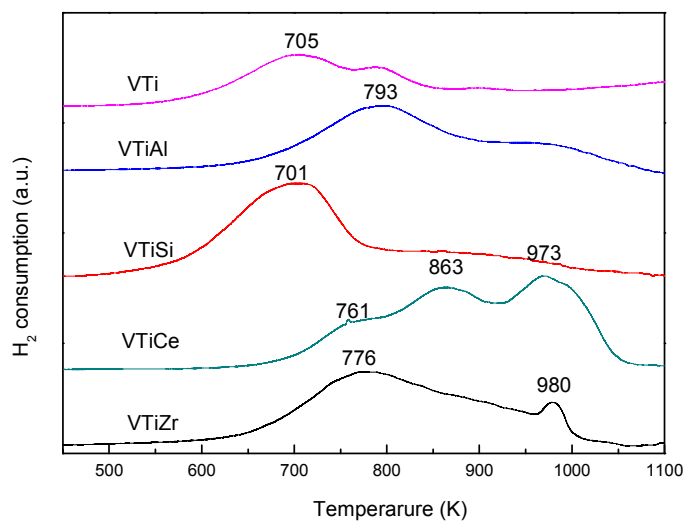


Fig. 5.

